Available online at www.sciencedirect.com
SCIENCE DIRECT®
ELSEVIER
Physica D 187 (2004) 253–267
PHYSICA D
www.elsevier.com/locate/physd

Time-reversible deterministic thermostats

Wm.G. Hoover[a,b,*], Kenichiro Aoki[c], Carol G. Hoover[b], Stephanie V. De Groot[a]

[a] *Department of Applied Science, University of California at Davis/Livermore, Livermore, CA 94551-7808, USA*
[b] *Methods Development Group, Lawrence Livermore National Laboratory, Livermore, CA 94551-7808, USA*
[c] *Department of Physics, Keio University, 4-1-1 Hiyoshi, Kohoku-ku, Yokohama 223-8521, Japan*

Abstract

Seven different time-reversible deterministic thermostats are considered here and applied to a simple particle-based nonequilibrium heat-flow problem. This approach is robust. Results for all these different thermostats agree rather well for system widths of ten particle diameters or more. The simplest of the thermostats is the Gauss–Nosé–Hoover thermostat, based on kinetic-energy control. Higher moments of the particle momenta can be controlled by extensions of this idea involving as many as three additional thermostat variables. Generalizations of the deterministic thermostats suited to simulating "stochastic" and "Brownian" dynamics are discussed here too.

Keywords: Nonequilibrium; Molecular dynamics; Heat flow; Thermostats

1. Introduction

The traditional Hamiltonian approach to classical particle mechanics has no explicit tie to temperature, but the temperature concept is required for a *thermodynamic* description of mechanical simulations. At a minimum the temperature concept requires averaging, either over an ensemble or over time. It is a *statistical* concept. One could imagine elaborate mechanical models of thermostats—models involving many degrees of freedom coupled together with "realistic" forces. It is fortunate that such detailed complicated models of thermostats are unnecessary. Thirty years of particle simulations have shown that very simple models, with only a few degrees of freedom, can fill the need for temperature control in mechanical systems. With a little care even very simple systems—a single hard disk or a single harmonic oscillator—can be coerced into the ergodic behavior which makes their long-time-averaged behavior independent of initial conditions.

Maxwell and Boltzmann's kinetic theory implies that the kinetic-theory temperature T_{KT} is necessarily defined by the average kinetic energy of any typical Cartesian degree of freedom, relative to a comoving corotating frame:

$$T_{KT} \equiv \frac{\langle p^2 \rangle}{mk}.$$

The average need not be carried out over a large number of particles. Sometimes, as in the oscillator example worked out in Section 7, a single particle, or even a single degree of freedom, can be held to a *time-averaged*

* Corresponding author. Tel.: +1-925-422-9787.
E-mail address: biru@midway.llnl.gov (Wm.G. Hoover).

0167-2789/$ – see front matter © 2003 Elsevier B.V. All rights reserved.
doi:10.1016/j.physd.2003.09.016

temperature by chosing an appropriate thermostatting force. Mechanics can be generalized, to "thermomechanics," by incorporating this time-averaged kinetic energy mechanical definition directly into the equations of motion [1–3]. There have been corresponding fruitful efforts for quantum systems [4,5].

During the last 30 years thermomechanics, with the kinetic-theory temperature T_{KT} included, has been used to simulate and analyze hydrodynamic nonequilibrium processes. Here we explore and compare representative computational "thermostats" based on this concept. These thermostats have been used to constrain or control the kinetic temperatures of mechanical systems.

The investigations one pursues and the conclusions one reaches depend very much on one's perspective. Computational thermostats can play either of two important roles: (i) providing smooth boundary conditions on flows, or (ii) providing models for the complexity of real-world heat transfer. Though we stress the first of these applications here, we certainly agree that the second, models for real-world heat transfer, is ripe for exploration. The subject of thermostats has not only aesthetic, philosophical, and pedagogical aspects, but also practical ones. The simplicity, efficiency, and the number dependence of numerical simulations, particularly in systems far from equilibrium, all hinge on making a good thermostat choice.

We begin by reviewing the simplest temperature definition, that based on the mean squared momentum [6]. Gibbs' entropy and the canonical ensemble are discussed next. We then consider several more complicated types of computational thermostats [7–11], all of them deterministic and time-reversible. We focus on their relative success in imposing smooth thermal boundary conditions on prototypical nonequilibrium systems.

We do not choose to belabor here the required ergodicity of the underlying mechanics, without which the results would depend on the initial conditions. We also do not reproduce the analyses necessary to show that the thermostats considered here are all compatible with corresponding Gibbs' ensembles. These topics are addressed in the references, among which [8] provides a particularly thorough and readable treatment. See also the contributions of Ebeling, Evans, and Klages to these proceedings.

We point out that the conventional stochastic approaches to model the Langevin equation or Brownian dynamics could just as well be based on deterministic chaos. To illustrate the variety of deterministic thermostats considered here we follow Evans and Holian's lead [12] in applying several representative types to a single far-from-equilibrium problem. Holian and Evans studied the viscosity of a dense fluid. Here we study heat conduction in an idealized two-dimensional solid. Our conclusions make up the final section.

2. Identifying temperature with kinetic energy

Temperature is the state variable which distinguishes thermodynamics and hydrodynamics from mechanics. Thermodynamic temperature is typically, and most usefully, *defined* in terms of the average pressure $\langle P \rangle$ exerted by an N-body ideal-gas thermometer (which *defines* the ideal-gas temperature T_{IG}) confined within a volume V [6]:

$$T_{IG} \equiv \frac{\langle P \rangle V}{Nk}.$$

An elementary kinetic-theory calculation computes the rate of momentum transfer from a gas to a fixed container wall. Because the collision rate and the momentum transfer per collision are both proportional to the velocity normal to the wall, the average pressure can thus be simply related to the mean squared momentum.

Although this derivation envisions a large number of particles interacting with their container, the same expression can make sense even for a single particle. See for instance, the two doubly thermostatted oscillator models elaborated in Section 7. Though "temperature" has been characterized by kinetic energy from the earliest days of kinetic theory, the reasons why are seldom articulated. Briefly, the thermal equilibration of a single degree of freedom, brought

about by collisions with a Maxwell–Boltzmann ideal gas (the ideal-gas thermometer), can be analyzed with kinetic theory. The single degree of freedom eventually attains the Maxwell–Boltzmann velocity distribution appropriate for its mass. The kinetic-theory temperature T_{KT} of this degree of freedom (based on the long-time-averaged kinetic energy) reaches the ideal-gas temperature T_{IG}, so that

$$\frac{\langle p_x^2 \rangle}{mk} \equiv T_{KT} = T_{IG}.$$

This mechanical ideal-gas kinetic-theory definition of temperature is far better than an alternative based on thermodynamic entropy

$$T_{bad} \equiv \left(\frac{\partial E}{\partial S} \right)_V$$

because entropy, at least the Gibbs' entropy S_{Gibbs} accessible through statistical mechanics, is a problematic concept far from equilibrium. This is because the nonequilibrium phase-space distributions are typically strange-attractor *fractal* distributions, with *singular* probability densities f [1–3,11,13,14] rather than the smooth canonical distributions which describe equilibrium. As a result, the usual statistical–mechanical formulation of the equilibrium entropy, expressed in terms of the phase-space probability density,

$$S_{Gibbs} \equiv -k \langle \ln f \rangle,$$

can give a *divergent* value for the entropy, in nonequilibrium steady states [13–15]:

$$\frac{S_{Noneq}}{k} \to -\infty.$$

In practice the "long-time-limit" averages that "steady states" require converge relatively rapidly. The heat-flow problem discussed in Section 9 illustrates this rapid convergence.

The kinetic-theory temperature definition, which corresponds also to an ideal-gas thermometer, $T_{KT} = \langle p_x^2 \rangle / mk$ carries over to any equilibrium classical system, gas, liquid, solid, or a multiphase mixture. Kinetic-theory temperature can be used both at and away from equilibrium. At equilibrium, where entropy is a valid concept, the maximization of entropy invariably leads to the Maxwell–Boltzmann "Gaussian" distribution of momenta:

$$f(p) \propto e^{-p^2/2mkT}.$$

Equilibrium is expected to result whenever the number of degrees of freedom is large, or whenever the system in question—even a single molecule—interacts with a suitable heat reservoir.

In Hamiltonian mechanics the time-dependent variables are the generalized coordinates $\{q\}$ and their conjugate momenta $\{p\}$. The motion of an isolated system, given by the set of first-order differential equations:

$$\left\{ \dot{q} = +\frac{\partial H}{\partial p}, \dot{p} = -\frac{\partial H}{\partial q} \right\}$$

is isoenergetic,

$$\dot{H} = \sum \left[\dot{q} \frac{\partial H}{\partial q} + \dot{p} \frac{\partial H}{\partial p} \right] = \sum \left[\frac{\partial H}{\partial p} \frac{\partial H}{\partial q} - \frac{\partial H}{\partial q} \frac{\partial H}{\partial p} \right] \equiv 0,$$

rather than isothermal, and temperature does not enter the motion equations explicitly.

At thermal equilibrium, with the system no longer isolated, it is traditional to imagine a weak coupling of system to thermostat. The coupling is sufficiently weak that the thermostat's Maxwell–Boltzmann momentum distribution

is undisturbed. In the absence of such an equilibrium, the momentum distribution is seldom known in advance and the system "temperature," if it still defined in terms of $\langle p^2 \rangle$, can easily deviate from the temperature T of the external reservoir to which the system is coupled. "Temperature jumps" are typical at the boundaries of strongly nonequilibrium systems [16,17].

In the early days of molecular dynamics it was natural to rescale the particle momenta sufficiently often, in order to keep the "kinetic temperature" constant. At the end of a computational timestep dt, where the particle momenta $\{p(t)\}$ have become $\{p(t + dt)\}$, each of the new momenta is multiplied by a rescaling constant to give the new set $\{p'(t + dt)\}$ with the *same* kinetic energy as at the previous time t:

$$p' \propto p(t + dt) \rightarrow \sum \frac{p'^2}{m} = \sum \frac{p^2(t)}{m} = \#kT_{\rm KT},$$

where # is the number of thermostatted degrees of freedom. Certainly this constrained "isokinetic dynamics" constitutes the simplest deterministic and time-reversible (for a sufficiently small timestep dt) "thermostat." Although neither determinism nor reversibility is strictly required, both are advantageous in simplifying the interpretation of results and in making simulations reproducible. With the natural tendency toward more elaborate approaches there are by now *many* different thermostat types in use [7–11]. Flexibility in thermostatting is highly desirable when it is necessary to model complicated experimental situations with, for example,

$$T_{\rm electronic} \neq T_{\rm nuclear} \neq T_{\rm radiation}.$$

On the other hand, our interest here is simplicity, so that the models we consider are more limited in scope. All of them have been developed in order to describe the thermal properties of classical point particles.

3. Identifying entropy with phase volume

Gibbs' and Boltzmann's equilibrium statistical mechanics can be based on the identification of the macroscopic entropy with the accessible microscopic phase volume:

$$\frac{S}{k} = -\langle \ln f \rangle = -\iint f(q, p) \ln f(q, p) \prod [dq\, dp].$$

This bridge between the macroscopic and microscopic points of view establishes their equivalence for equilibrium situations. Numerical simulations have shown that extending this same relation to nonequilibrium stationary states is not possible because those states are characterized by *fractal* distributions, corresponding to divergent entropies [13–15,17,18]. A long range goal of the present research effort is to establish, as clearly as possible, the general characteristics of nonequilibrium steady states and their phase-space distributions.

4. Gauss' instantaneous thermostats

It has been known for more than 20 years that the instantaneous momentum-scaling isokinetic thermostat is exactly the same as that derived from mechanics according to Gauss' principle. Gauss' principle (of least constraint, 1828) states that the least possible constraint force should be used with "least" construed in the sense of minimizing the summed-up squares of all constraint forces affecting the system:

$$\delta \sum \frac{F_c^2}{2m} \equiv 0,$$

where δ indicates an infinitesimal variation over all nearby sets of constraint forces which satisfy the desired constraints. The variation vanishes for the "least" constraint in this sense. According to Gauss' principle, an instantaneous constraint on the kinetic energy, $\sum p^2/2m$, is "best" accomplished by adding a constraint force $-\zeta p$ which is linear in the momenta. Constraint forces which additionally tend to rotate, rather than just stretch or shrink, the momenta give a larger sum $\sum F_c^2/2m$. If the fourth or sixth moment were constrained instead, then a cubic or quintic constraint force would result. In the cubic case, Gauss' principle gives

$$\dot{p} = F(q) - \zeta p^3, \quad \zeta = \frac{\sum F(q)p^3}{\sum p^6}.$$

Why is controlling the second moment $\langle p^2 \rangle$ the best choice? In addition to simplicity, the second moment is the best choice because $\sum p^2$ is precisely constant for the ideal-gas thermometer in the absence of external interactions. For the ideal gas the energy is completely kinetic. Other moments of the gas fluctuate, with the fluctuations dying away only in the infinite-system limit. Thus alternative thermostats, which fix $\langle p^4 \rangle$ or $\langle p^6 \rangle$ rather than $\langle p^2 \rangle$ are not so desirable on physical grounds. We will compare only the two simplest moment-based examples here, those based on $\langle p^2 \rangle$ and on $\langle p^4 \rangle$.

5. Gibbs' canonical distribution: Nosé–Hoover thermostats

Gibbs showed (as did also Boltzmann, and at about the same time, 1883) that the Maxwell–Boltzmann distribution of the momenta applies to all classical systems at equilibrium, to dense gases, to liquids, and to solids, just as the distribution applies to the dilute gases studied in kinetic theory. Gibbs approached the problem from the statistical point of view, where the ensemble-averaged entropy of Section 3,

$$\frac{S}{k} = -\langle \ln f(q, p) \rangle,$$

plays a central role because its maximum defines equilibrium.

Just a century later, in 1984, Nosé [7] discovered that Gibbs' canonical distribution can be obtained directly from dynamics, without any mention of entropy. Nosé's canonical-ensemble dynamics follows from a Hamiltonian based on the conventional one (with kinetic energy K and potential energy Φ), but includes an additional pair of canonically conjugate variables, s and p_s. The desired temperature T appears as a parameter in Nosé's Hamiltonian. The new variables can then impose the canonical distribution characteristic of the temperature T on the dynamics. The simplest derivation of Nosé's new dynamics can be found, almost buried, in one of the Nosé's 1984 papers [7]. Start with the special Hamiltonian $H_{\text{Nosé}}$:

$$H_{\text{Nosé}} \equiv \frac{K}{s} + s\left[\Phi + \frac{p_s^2}{2\#kT\tau^2} + \#kT \ln s\right] \equiv 0.$$

Here K is the thermostatted kinetic energy, T the constant "target" temperature, $\#$ the number of thermostatted degrees of freedom, and τ a relaxation time, which determines the frequency of temperature fluctuations. Although one could omit the $\#$ in the denominator of the thermostat kinetic energy we feel it is advantageous to include it. This choice shows explicitly how the influence of the thermostat $\propto 1/\sqrt{\#}$, decreases as the number of degrees of freedom thermostatted increases.

The Hamiltonian equations of motion which follow by differentiating $H(q, p, s, p_s)$ can be simplified by making the replacements

$$\left\{\frac{p}{s} \to p\right\}, \quad \frac{\dot{s}}{s} \to \zeta$$

with the result

$$\left\{\dot{q} = \frac{p}{m},\ \dot{p} = -\nabla\Phi - \zeta p\right\}, \qquad \dot{\zeta} \equiv \frac{\dot{p}_s}{\#\tau^2 kT} = \sum \frac{(p^2/mkT) - 1}{\#\tau^2}.$$

The equation of motion for the friction coefficient ζ is an example of "integral feedback." It has a simple interpretation. Whenever the kinetic energy exceeds the target value of $(1/2)kT$ (for each thermostatted degree of freedom) the friction is increased, so as to extract more energy. Whenever the kinetic energy is less than the target value, the friction becomes more negative. Negative friction causes the system to heat while positive friction causes it to cool off. For systems sufficiently chaotic as to fill their energy shells, the additional "friction coefficient" forces $\{-\zeta p\}$ generate the complete generalized canonical distribution:

$$f(q, p, \zeta) \propto \mathrm{e}^{-H/kT}\,\mathrm{e}^{-\#\tau^2\zeta^2/2}.$$

Otherwise, they generate only a portion of it.

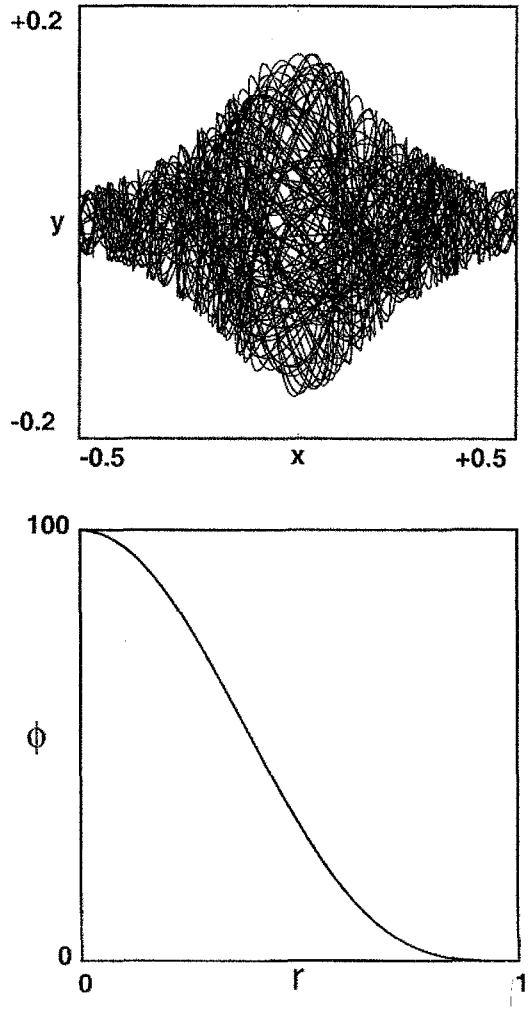

Fig. 1. Isoenergetic trajectory of a single chaotic ergodic particle in a periodic cell with fixed particles at the cell corners. The interparticle pair potential is a smooth repulsive potential, $\phi(r) = 100(1 - r^2)^4$, for $r < 1$, which has three continuous derivatives, and is shown here.

Here Nosé's friction coefficient ζ has units of inverse time. Because, in what follows, we will use a variety of power-law thermostats, it is a little simpler to choose a *dimensionless* friction coefficient:

$$(\zeta \to \tau\zeta) \to \dot{\zeta} \equiv \frac{\dot{p}_s}{\#\tau kT}.$$

The corresponding equations of motion and distribution function then become:

$$\left\{ \dot{q} = \frac{p}{m}, \dot{p} = -\nabla\Phi - \frac{\zeta p}{\tau} \right\}, \qquad \dot{\zeta} = \sum \frac{(p^2/mkT) - 1}{\#\tau}, \qquad f(q, p, \zeta) \propto \mathrm{e}^{-H/kT} \mathrm{e}^{-\#\zeta^2/2},$$

assuming that the dynamics is sufficiently mixing for ergodicity. With this dimensionless choice for ζ it is noteworthy that the phase-space distribution function $f(q, p, \zeta)$ is *independent* of the relaxation time τ. The simplest system with continuous forces which fills all the requirements for ergodicity is probably the one-body cell-model problem whose solution is shown in Fig. 1.

6. Other deterministic thermostats

Once temperature is defined in terms of the second moment, $T \equiv \langle p_x^2 \rangle / mk$, it is evident that a "good" thermostat must impose this value on the velocity distribution. At equilibrium a variety of thermostats can do this. The oldest of them is probably Langevin's, which adds both a drag force, $-\gamma p$, and a "random fluctuating force" to the equations of motion. In Langevin's equation the friction coefficient γ is a phenomenological constant. By choosing the corresponding amplitude of the random force properly the drag can be offset, on the average, resulting in the correct second-moment temperature. Away from equilibrium the Langevin approach fails to constrain the temperature $\propto \langle p^2 \rangle$ to the target value. It lacks the necessary "feedback" to respond to irreversible heating. Nosé's integral-feedback approach has the distinct advantage that it provides the desired second moment exactly, even far from equilibrium.

There have been many generalizations of Nosé's ideas. This work has now spanned two decades [8,12,19]. When three or more thermostat variables "demons" are added to the free-particle equations of motion it is even possible to reproduce Brownian motion, with normal diffusion, and with an equilibrium Maxwell–Boltzmann velocity distribution:

$$\langle r^2 \rangle \propto t, \qquad \langle f(p) \rangle \propto \mathrm{e}^{-p^2/2mkT}.$$

A family of thermostats using higher powers of the friction coefficient leads, at equilibrium, to Gaussian distributions of the corresponding friction variables [1,8]:

$$\dot{p} = F - \frac{z^3 p}{\tau}, \quad \dot{z} = \frac{(p^2/mkT) - 1}{\tau} \to f(z) \propto \mathrm{e}^{-z^4/4};$$

$$\dot{p} = F - \frac{z^5 p}{\tau}, \quad \dot{z} = \frac{(p^2/mkT) - 1}{\tau} \to f(z) \propto \mathrm{e}^{-z^6/6}.$$

For simplicity we continue to choose the friction coefficients to be dimensionless. We include a characteristic relaxation time τ which governs the rate at which control is applied. This combination of choices gives a phase-space distribution function independent of τ, though useful simulations require a good choice of the response time τ.

It is easy to show, by making a change of variable,

$$z^4 \text{ or } z^6 \propto \zeta^2,$$

that all these alternatives give an equilibrium phase-space distribution identical to that obtained with Nosé's second-moment control. Nevertheless, because the dynamical equations are different, the various power-law thermostats can produce different predictions away from equilibrium, as we see explicitly in Section 9.

Nosé's thermostat controls the difference between the instantaneous and target values of the temperature. Additional feedback variables can be added, as in the simplest of Tuckerman's chain-thermostat schemes [10,19]:

$$\dot{p} = F(q) - \frac{\zeta p}{\tau}, \qquad \dot{\zeta} = \frac{((p^2/mkT) - 1) - \xi\zeta}{\tau}, \qquad \dot{\xi} = \frac{\zeta^2 - 1}{\tau}.$$

This scheme can provide an ergodic Gaussian distribution for the harmonic oscillator. If we choose the mass and force constant equal to unity, for example, the phase-space distribution function is a Gaussian in the four-dimensional "extended" phase space which includes the friction coefficients ζ and ξ:

$$F(q) = -q \to f(q, p, \zeta, \xi) \propto \mathrm{e}^{-[(q^2+p^2)/2kT]}\, \mathrm{e}^{-(\zeta^2+\xi^2)/2}.$$

Longer chains of thermostat variables can be used too [10].

Friction coefficients can be used to control other velocity moments. In Section 4 we pointed out that the fourth moment could be controlled using Gauss' principle, giving a cubic constraint force. Another possibility, closely resembling Nosé's integral feedback and replicating the canonical momentum distribution is

$$\dot{p} = F(q) - \frac{\xi[p^3/mkT]}{\tau}, \qquad \dot{\xi} = \frac{p^4/(mkT)^2}{\tau} - \frac{3[p^2/mkT]}{\tau}.$$

It is quite practical to combine this fourth-moment control with conventional Nosé–Hoover thermostatting so as to control both the second and fourth moments simultaneously [9].

A variety of other thermostats can be tried out. Other moments can be controlled, but, because the second moment is uniquely conserved by an ideal-gas thermometer, it seems preferable to use the second. Before embarking on a comparison of the methods let us briefly consider stochastic thermostats too.

7. Langevin equation thermostats

The Langevin equation [20,21] provides a phenomenological model of thermal equilibration. It is a relic predating both computers and our current knowledge of deterministic chaos. The Langevin equation is still implemented today, by using deterministic random number generators to model the "stochastic forces" which are a necessary ingredient. The Langevin equation includes a somewhat unaesthetic mixture of deterministic forces, both irreversible and reversible, along with a random statistical (or "stochastic") force. Both the "drag" force, linear in the velocity, and the stochastic force are irreversible, while the systematic force $F(q)$ is time-reversible.

The Langevin equation

$$\dot{p} = F(q) - \frac{p}{\tau} + F_{\mathrm{random}}(t, \mathrm{d}t),$$

requires some interpretation in order that the random forces be well-defined in numerical simulations. In a simulation with finite timestep $\mathrm{d}t$ the effect of constant drag and random forces during a step can be modeled by an adjustment of the momentum at the end of the timestep:

$$p(t + \mathrm{d}t) = p(t)\, \mathrm{e}^{-\mathrm{d}t/\tau} + F_{\mathrm{random}}(t, \mathrm{d}t)\, \mathrm{d}t.$$

The argument below can be used to show that the contribution of $F(q)\,\mathrm{d}t$ can be omitted relative to the singular contribution $\propto \sqrt{\mathrm{d}t}$ from the random force. Ignoring $F(q)$ and imposing the requirements that (i) the mean value

of p^2 be stationary and (ii) the mean value of the random force vanish gives an identity (for $dt \ll \tau$):

$$\langle p(t+dt)^2\rangle = \left\langle \left[p(t)\left(1-\frac{dt}{\tau}\right) + F_{\text{random}}\, dt\right]^2\right\rangle$$
$$= \langle p(t)^2\rangle\left(1-2\frac{dt}{\tau}\right) + dt^2\langle F^2_{\text{random}}\rangle \to mkT \equiv \langle p^2\rangle = \frac{\langle F^2_{\text{random}}\rangle \tau\, dt}{2}.$$

Thus the random forces must diverge (as $\sqrt{1/dt}$), and must consequently give rise to vanishing impulses (proportional to $\sqrt{dt}$) as the computational timestep dt is reduced. There is a voluminous history of simulations of this kind in which the random forces are selected from a Gaussian distribution consistent with both the assumed drag force $-p/\tau$ and the assumed temperature. If the drag force is omitted then some other mechanism (a harmonic restoring force is the simplest example) is required to localize the diffusion in velocity and coordinate space.

At the Dresden Workshop Holger Kantz' presentation, "Replacing Fast Chaotic Degrees of Freedom by Random Noise: a Formally Exact Approach" demonstrated that the Lorenz attractor, with a distribution far from Gaussian, can be used as a stochastic noise source for the Langevin equation.

Rather than use Gaussian random numbers we could model the Langevin random forces with a single oscillator coordinate q generated with the minimum number of differential equations required for an ergodic Gaussian distribution. Let us choose all the free parameters describing the controlled oscillator equal to unity. One convenient set of equations generating Gaussian distributions for (q, p, ζ, ξ) is based on Tuckerman's chain idea [10]:

$$\dot q = p, \qquad \dot p = -q - \zeta p, \qquad \dot\zeta = p^2 - 1 - \xi\zeta, \qquad \dot\xi = \zeta^2 - 1.$$

These oscillator equations, like those of the system immediately following and detailed in [18], are compatible with Gibbs' canonical distribution [1,8]. Computation reveals that the two sets are also ergodic, so that the results obtained do not depend on initial conditions.

The oscillator coordinate is not the only possibility for "random" forces. The oscillator momentum p or either of the two friction coefficients, ζ and ξ, could also be used as surrogate forces. Any of these choices will guarantee that the ensemble-averaged Langevin coordinate obeys a diffusion equation. The diffusion rate can be controlled by a proper scale choice of the surrogate forces. In the simplest case, an equilibrium Gaussian distribution with unit mean squared values of all the variables, the average time rates of change of the four variables are different:

$$\langle \dot q^2\rangle = \langle p^2\rangle = 1, \qquad \langle \dot p^2\rangle = \langle q^2 + \zeta^2 p^2\rangle = 2, \qquad \langle \dot\zeta^2\rangle = \langle p^4 - 2p^2 + 1 + \zeta^2\xi^2\rangle = 3,$$
$$\langle \dot\xi^2\rangle = \langle \zeta^4 - 2\zeta^2 + 1\rangle = 2.$$

The doubly thermostatted oscillator of Ref. [18]:

$$\dot q = p, \qquad \dot p = -q - \zeta p - \xi p^3, \qquad \dot\zeta = p^2 - 1, \qquad \dot\xi = p^4 - 3p^2,$$

though it has exactly the same phase-space distribution, provides very different time-averaged rates of change:

$$\langle \dot q^2\rangle = \langle p^2\rangle = 1, \qquad \langle \dot p^2\rangle = \langle q^2 + \zeta^2 p^2 + \xi^2 p^6\rangle = 17, \qquad \langle \dot\zeta^2\rangle = \langle p^4 - 2p^2 + 1\rangle = 2,$$
$$\langle \dot\xi^2\rangle = \langle p^8 - 6p^6 + 9p^4\rangle = 42.$$

8. Other stochastic thermostats and maps

Other types of statistical simulations can be based on occasional selections of thermostatted momenta from a suitable equilibrium thermal distribution. This replacement is usually carried out at some fixed geometric "boundary"

of the simulated system. This procedure is, like the Langevin equation itself, somewhat unaesthetic because the corresponding forces are impulsive, giving *discontinuities* in the velocities of the thermostatted particles. The additional drawback of adopting a boundary dynamics which is not time-reversible can be avoided by using a time-reversible deterministic map (the Baker Map has been used) to determine the post-collision momenta [11]. A defect of this map approach is the apparent loss of connection between entropy production and phase-space volume due to ambiguities in defining the "reservoir temperature" away from equilibrium. See Rainer Klages' very interesting contribution to this workshop.

In the usual stochastic approach, a particle reaching the boundary is reinjected with a momentum chosen from the one-sided distribution proportional to $p\,e^{-p^2/2mkT}$. This scheme is somewhat unphysical in that the incoming temperature has no influence on the outgoing one. The Langevin equation and such a stochastic dynamics share the twin disadvantages of (i) time-*irreversible* microscopic equations along with (ii) trajectories which are *discontinuous* in momentum space. The latter difficulty complicates differential stability analyses. Another consequence of forsaking feedback is that the "thermostatted particle" described by Langevin or stochastic dynamics exhibits a temperature intermediate between the desired one and that of the nonequilibrium system with which the particle interacts.

9. Numerical comparison of thermostats

Let us compare a variety of thermostats in simulating a strongly nonequilibrium system. We use the thermostats to constrain the temperatures of four boundary particles on the left (cold) and four boundary particles on the right (hot) where the two boundaries enclose a model 4×4 Newtonian system sandwiched between them. The boundary particles obey special thermostatted equations of motion, as summarized below, while the particles in the Newtonian region obey standard conservative classical mechanics.

See Fig. 2 for an illustration of a complete thermostatted 6×4 two-dimensional system with boundary temperatures of $kT_C = 0.005$ and $kT_H = 0.015$. The model shown in the figure is a tethered square 4×4 lattice which reacts to the a temperature gradient provided by two similarly tethered, but thermostatted, 1×4 reservoir regions. "Free" boundaries are used on all four sides of the system. All $4 + 16 + 4 = 24$ particles have unit mass and are tethered to lattice sites separated from their nearest neighbors sites by unit distance. The equations of motion for the 16 interior conventional Hamiltonian particles are

$$\left\{ \dot{q} = \frac{p}{m}, \dot{p} = -\nabla\Phi \right\},$$

where the potential energy Φ contains all 38 (20 "horizontal" and 18 "vertical") nearest-neighbor Hooke's law terms $(|\Delta r_{ij}|-1)^2/2$ as well as the 24 individual-particle tethering terms of the form $\delta r_i^4/4$. This particular heat-flow model is notable for demonstrating very clearly that the phase-space dimensionality loss—relative to the equilibrium phase-space dimensionality—of its nonequilibrium phase-space strange attractors can greatly exceed the dimensionality associated with the thermostatted boundary particles [18].

Here we compare seven distinct deterministic and time-reversible treatments of the eight thermostatted particles on the two sides of the system. To simplify notation here we use $\langle \cdots \rangle$ to indicate an average over the four cold or hot particles making up one of the two thermostats. Here are two examples—note that the sums, over four thermostatted particles, include contributions from eight Cartesian degrees of freedom each:

$$\langle Fp^3 \rangle \equiv \frac{1}{8} \sum [F_x(i) p_x(i)^3 + F_y(i) p_y(i)^3], \qquad \langle p^4 \rangle \equiv \frac{1}{8} \sum [p_x(i)^4 + p_y(i)^4].$$

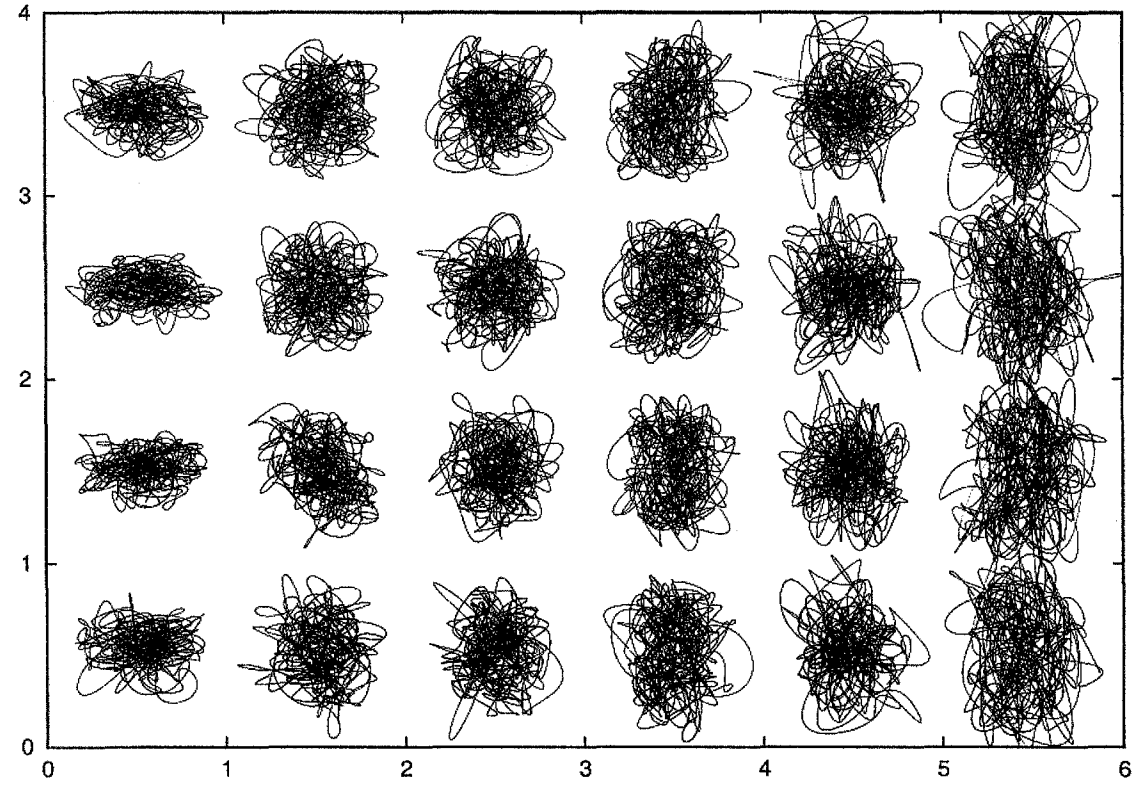

Fig. 2. Geometry of a 24-particle two-dimensional steady-state system. The leftmost four particles are cold and the rightmost four hot. The remaining 16 particles obey conventional Hamiltonian mechanics. For clarity in illustrating the trajectories, the cold and hot temperatures of the thermostatted particles for this figure were imposed using Nosé–Hoover dynamics with $T_C = 0.005$ and $T_H = 0.015$, two orders of magnitude smaller than those used to generate the data in Table 1.

Using this $\langle \cdots \rangle$ notation the seven thermostat treatments have the following forms:

(i) Gauss' instantaneous p^2 control:

$$\dot{p} = F - \zeta_1 p, \quad \zeta_1 = \frac{\langle Fp \rangle}{\langle p^2 \rangle};$$

(ii) Gauss' instantaneous p^4 control:

$$\dot{p}_x = F_x - \zeta_2 p_x^3, \qquad \dot{p}_y = F_y - \zeta_2 p_y^3, \quad \zeta_2 = \frac{\langle Fp^3 \rangle}{\langle p^6 \rangle};$$

(iii) Nosé–Hoover p^2 control:

$$\dot{p} = F - \frac{\zeta_3 p}{\tau}, \quad \dot{\zeta}_3 = \frac{(\langle p^2 \rangle / mkT) - 1}{\tau};$$

(iv) Cubic p^4 control:

$$\dot{p}_x = F_x - \zeta_4 \frac{p_x^3/mkT}{\tau}, \qquad \dot{p}_y = F_y - \zeta_4 \frac{p_y^3/mkT}{\tau}, \qquad \dot{\zeta}_4 = \frac{\langle p^4 \rangle / (mkT)^2 - 3(\langle p^2 \rangle / mkT)}{\tau};$$

Table 1
Cold and hot temperatures, the overall heat transfer rate $\dot{Q}_H = -\dot{Q}_C$, and fourth-moment ratios $\langle p^4\rangle/\langle p^2\rangle^2$ for the seven deterministic time-reversible thermostatted heat flows described in Section 9

Type	T_{Cx}	T_{Cy}	T_{Hx}	T_{Hy}	$\dot{Q}_H$	R_{Cx}	R_{Cy}	R_{Hx}	R_{Hy}
(i)	0.52	0.48	1.48	1.52	0.14	2.41	2.48	2.42	2.40
(ii)	0.59	0.56	1.70	1.70	0.13	2.20	2.27	2.33	2.32
(iii)	0.52	0.48	1.49	1.51	0.18	2.96	3.06	3.40	3.38
(iv)	0.55	0.53	1.36	1.39	0.15	2.73	2.82	3.29	3.24
(v)	0.52	0.48	1.49	1.51	0.19	2.93	3.07	3.01	2.98
(vi)	0.55	0.50	1.45	1.49	0.20	3.04	3.13	3.09	3.06
(vii)	0.52	0.48	1.49	1.51	0.19	2.99	3.11	3.26	3.22

These data are for 24-particle (6 × 4) systems with 4 cold particles, 16 Newtonian particles, and 4 hot particles, as is illustrated in Fig. 2. Fifty million fourth-order Runge–Kutta timesteps (dt = 0.002) were used in each case.

(v) Hoover–Holian p^2 and p^4 control:

$$\dot{p}_x = F_x - \frac{\zeta_5 p_x + \xi_5(p_x^3/mkT)}{\tau}, \qquad \dot{p}_y = F_y - \frac{\zeta_5 p_y + \xi_5(p_y^3/mkT)}{\tau},$$
$$\dot{\zeta}_5 = \frac{(\langle p^2\rangle/mkT) - 1}{\tau}, \qquad \dot{\xi}_5 = \frac{\langle p^4\rangle/(mkT)^2 - 3(\langle p^2\rangle/mkT)}{\tau};$$

(vi) Tuckerman p^2 chain control:

$$\dot{p} = F - \frac{\zeta_6 p}{\tau}, \qquad \dot{\zeta}_6 = \frac{(\langle p^2\rangle/mkT) - 1 - \#\zeta_6\xi_6}{\tau}, \qquad \dot{\xi}_6 = \frac{\#\zeta_6^2 - 1}{\tau};$$

(vii) Cubic (ζ^3) p^2 control:

$$\dot{p}_x = F_x - \frac{\zeta_7^3 p_x}{\tau}, \qquad \dot{p}_y = F_y - \frac{\zeta_7^3 p_y}{\tau}, \qquad \dot{\zeta}_7 = \frac{(\langle p^2\rangle/mkT) - 1}{\tau}.$$

The last five of these thermostats incorporate one or more relaxation times $\{\tau\}$. For simplicity we have chosen all these times equal to unity in the numerical work. To avoid prejudicing the results we have also chosen for investigation a problem in which the mean temperature values, $\langle p_x^2\rangle \simeq \langle p_y^2\rangle$, are of order unity throughout the system. Tables 1–3 correspond to specified boundary temperatures of $kT_C = 0.5$ and $kT_H = 1.5$. They show the mean values of the kinetic temperatures, $\langle p_x^2/mk\rangle$ and $\langle p_y^2/mk\rangle$, the overall heat flux, and the boundary values for

Table 2
Cold and hot temperatures, the overall heat transfer rate $\dot{Q}_H = -\dot{Q}_C$ and fourth-moment ratios $\langle p^4\rangle/\langle p^2\rangle^2$ for the seven deterministic time-reversible thermostatted heat flows described in Section 9

Type	T_{Cx}	T_{Cy}	T_{Hx}	T_{hy}	$\dot{Q}_H$	R_{Cx}	R_{Cy}	R_{Hx}	R_{Hy}
(i)	0.52	0.48	1.49	1.51	0.12	2.40	2.47	2.41	2.39
(ii)	0.60	0.56	1.72	1.70	0.12	2.20	2.28	2.31	2.32
(iii)	0.52	0.48	1.50	1.50	0.14	2.95	3.03	3.25	3.22
(iv)	0.55	0.52	1.42	1.42	0.13	2.77	2.85	3.18	3.17
(v)	0.52	0.48	1.49	1.51	0.14	2.95	3.06	3.01	2.99
(vi)	0.54	0.50	1.47	1.49	0.14	2.99	3.08	3.04	3.03
(vii)	0.52	0.48	1.49	1.51	0.14	2.96	3.07	3.16	3.13

These data are for 40-particle (10 × 4) systems with 4 cold particles, 32 Newtonian particles, and 4 hot particles. One hundred million fourth-order Runge–Kutta timesteps (dt = 0.002) were used in each case.

Table 3
Cold and hot temperatures, the overall heat transfer rate $\dot{Q}_H = -\dot{Q}_C$ and fourth-moment ratios $\langle p^4\rangle/\langle p^2\rangle^2$ for the seven deterministic time-reversible thermostatted heat flows described in Section 9

Type	T_{Cx}	T_{Cy}	T_{Hx}	T_{Hy}	$\dot{Q}_H$	R_{Cx}	R_{Cy}	R_{Hx}	R_{Hy}
(i)	0.51	0.49	1.50	1.50	0.089	2.39	2.44	2.40	2.39
(ii)	0.59	0.56	1.72	1.70	0.092	2.21	2.28	2.30	2.31
(iii)	0.51	0.49	1.49	1.51	0.092	2.96	3.01	3.13	3.13
(iv)	0.53	0.52	1.44	1.45	0.086	2.82	2.87	3.12	3.10
(v)	0.51	0.49	1.49	1.51	0.090	2.95	3.05	3.01	2.99
(vi)	0.52	0.50	1.48	1.49	0.094	2.98	3.05	3.02	3.01
(vii)	0.51	0.49	1.49	1.51	0.092	2.96	3.03	3.09	3.07

These data are for 72-particle (18×4) systems with 4 cold particles, 64 Newtonian particles, and 4 hot particles. Two-hundred million fourth-order Runge–Kutta timesteps ($dt = 0.002$) were used in each case.

the dimensionless ratio $R = \langle p^4\rangle/\langle p^2\rangle^2$ for each of the seven thermostat choices and for three different system sizes. R has the value $R = 3$ for Gaussian distribution.

We have chosen the run times long enough that the results quoted are accurate, with an uncertainty of order ± 1 in the last digit quoted. In addition to the results given in the tables we have investigated the dependence of the heat flow on the transverse width. The width dependence is quite regular, with the overall heat flow increasing with the system width, $Q \propto W$, as would be expected for any material obeying Fourier's law of heat conduction.

The appearance of the number of thermostatted degrees of freedom, #, in the chain control equations (vi) deserves special comment. It is dictated by Liouville's theorem [1,8,13], and is required even in the equilibrium case, for consistency with the generalized canonical distribution:

$$f_{eq} \propto e^{-H/kT} e^{-\#\zeta^2/2} e^{-\#\xi^2/2}.$$

Both friction coefficients, ζ and ξ, have fluctuations of order $1/\sqrt{\#}$ so that both the combinations $\#\zeta\xi$ and $\#\zeta^2$ are of order unity at equilibrium.

The nonequilibrium results in the tables show that the Gaussian fourth-moment thermostat (ii) delivers temperatures relatively far from the target values (0.5 and 1.5 in all seven examples). Only four of the seven thermostat choices, (i), (iii), (v), and (vii), reproduce the target temperatures,

$$\{T_C = \tfrac{1}{2}; T_H = \tfrac{3}{2}\},$$

exactly. The chain thermostat provides good transverse temperature control while missing the target temperature in the flow direction. The Nosé–Hoover thermostat (iii) produces nearly the same results as does the more elaborate simultaneous control of both the second and fourth moments (v). The more elaborate thermostats, (v) and (vi), provide very little tangible return for their additional complexity. The flow of heat varies by only a few percent from one thermostat type to another once the Newtonian part of the system is sufficiently long (see Table 3).

In addition to the simulations summarized in the tables we have carried out many others. A variant of the Nosé–Hoover form:

$$\dot{p} = F - \zeta^3 p - \xi p^3$$

provides temperatures and heat fluxes similar to those found using the approaches (iii), (v), and (vii) above. Because each of the feedback-based thermostats incorporates one or more characteristic relaxation times (here all chosen equal to unity) it is possible to "tune" them—even separately for the x and y directions—to reduce fluctuations or to improve their moments. The good agreement of the various choices shown in the tables indicates that the thermostat approach to nonequilibrium simulations is robust.

It is important to note that Tuckerman's original motion equations [10] are based on the difference, $p^2 - mkT$, rather than the ratio $(p^2/mkT) - 1$, and so give slightly different results away from equilibrium. Tuckerman's original equations also contain extraneous coordinates $\{q_\zeta, q_\xi\}$ associated with the friction coefficients and analogous to Nosé's s variable. Like s these extraneous coordinates *diverge* in nonequilibrium steady states and so are best avoided completely.

10. Conclusions and outlook

The precomputer stochastic thermostats can be replaced by a variety of simple and efficient deterministic thermostats, making precise reproducible time-reversible simulations possible, both at and away from equilibrium. The good agreement of the feedback thermostats, without any attempt to tune the many free parameters, indicates the overall usefulness of the thermostat approach. These results, for stationary heat flow, complement Holian and Evans' analogous investigation of shear flow [12].

The simplicity of thermostats based on the second moment of the velocity distribution and simply connected to irreversible thermodynamics recommends the use of Nosé–Hoover thermostats whenever possible. If the more elaborate multi-parameter thermostats are used it is necessary to check for consistency with Liouville's theorem. If it is desired to carry out Brownian dynamics a doubly thermostatted oscillator (two "demons" in the terminology of Bulgac and Kusnezov) can furnish a deterministic and reversible source of "stochastic" momenta.

Acknowledgements

This work was performed under the auspices of the United States Department of Energy through University of California Contract W-7405-Eng-48. SdG's work at Livermore was supported by a research apprenticeship in engineering grant from the Academy of Applied Science (Concord, New Hampshire). We very much appreciate the interest and encouragement of Aurel Bulgac, Dimitri Kusnezov, Harald Posch, Henk van Beijeren. Rainer Klages, Bob Dorfman, and Pierre Gaspard. Henk, Rainer, Bob, and Pierre helped to organize the International Workshop and Seminar on Microscopic Chaos and Transport in Many-Particle Systems (Dresden, August 2002) where this work was first discussed. At that same meeting several of our colleagues—Werner Ebeling, Denis Evans, Dennis Isbister, and Rainer Klages—presented work on thermostatted system from their own points of view. We were happy to have the opportunity to discuss thermostats with all of these colleagues, and recommend that the reader consult their contributions to these proceedings for a more comprehensive view of the field.

References

[1] W.G. Hoover, Computational Statistical Mechanics, Elsevier, Amsterdam, 1991.
[2] Wm.G. Hoover, Time Reversibility, Computer Simulation, and Chaos, World Scientific, Singapore, 1999, 2001.
[3] D.J. Evans, G.P. Morriss, Statistical Mechanics of Nonequilibrium Liquids, Academic Press, New York, 1990.
[4] A. Bulgac, G.D. Dang, D. Kusnezov, Dynamics of complex quantum systems: dissipation and kinetic equations, Physica E 9 (2001) 429–435.
[5] P.E. Blöchl, Second-generation wave-function thermostat for ab initio molecular dynamics, Phys. Rev. B 65 (2002) 104303.
[6] W.G. Hoover, B.L. Holian, H.A. Posch, Comment I on "Possible experiment to check the reality of a nonequilibrium temperature", Phys. Rev. E 48 (1993) 3196–3198.
[7] S. Nosé, A unified formulation of the constant temperature molecular dynamics methods, J. Chem. Phys. 81 (1984) 511–519.
[8] D. Kusnezov, A. Bulgac, W. Bauer, Canonical ensembles from chaos, Ann. Phys. 204 (1990) 155–185;
D. Kusnezov, A. Bulgac, W. Bauer, Canonical ensembles from chaos, Ann. Phys. 214 (1992) 180–218.

[9] Wm.G. Hoover, B.L. Holian, Kinetic moments method for the canonical ensemble distribution, Phys. Lett. A 211 (1996) 253–257.
[10] C.J. Martyna, M.L. Klein, M. Tuckerman, Nosé–Hoover chains—the canonical ensemble via continuous dynamics, J. Chem. Phys. 97 (1992) 2635–2643.
[11] K. Rateitschak, R. Klages, Lyapunov instability of two-dimensional many-body systems, Phys. Rev. E 65 (2002) 036209.
[12] D.J. Evans, B.L. Holian, The Nosé–Hoover thermostat, J. Chem. Phys. 83 (1985) 4069–4074.
[13] Wm.G. Hoover, Liouville's theorems, Gibbs' entropy, and multifractal distributions for nonequilibrium steady states, J. Chem. Phys. 109 (1998) 4164–4170.
[14] B.L. Holian, W.C. Hoover, H.A. Posch, Resolution of Loschmidt's paradox: the origin of irreversible behavior in atomistic dynamics, Phys. Rev. Lett. 59 (1987) 10–13.
[15] D. Ruelle, Smooth dynamics and new theoretical ideas in nonequilibrium statistical mechanics, J. Stat. Phys. 95 (1999) 393–468.
[16] K. Aoki, D. Kusnezov, Bulk properties of anharmonic chains in strong thermal gradients: nonequilibrium ϕ^4 theory, Phys. Lett. A 265 (2000) 250–256.
[17] K. Aoki, D. Kusnezov, Lyapunov exponents, transport, and the extensivity of dimensionality loss, nlin.CD/0204015, 10 April 2002.
[18] Wm.G. Hoover, H.A. Posch, K. Aoki, D. Kusnezov, Remarks on nonhamiltonian statistical mechanics: Lyapunov exponents and phase-space dimensionality loss, Europhys. Lett. 60 (2002) 337–341.
[19] Wm.G. Hoover, H.A. Posch, C.G. Hoover, Fluctuations and asymmetry via local Lyapunov instability in the time-reversible doubly thermostatted harmonic oscillator, J. Chem. Phys. 115 (2001) 5744–5750.
[20] N. Wax, Selected Papers on Noise and Stochastic Processes, Dover, New York, 1954.
[21] A. Bulgac, D. Kusnezov, Deterministic and time-reversal invariant description of Brownian motion, Phys. Lett. A 151 (1990) 122–128.